

Research



Article submitted to journal

Subject Areas:

xxxxx, xxxxx, xxxx

Keywords:

xxxx, xxxx, xxxx

Author for correspondence:

P.H. Trinh

e-mail: trinh@maths.ox.ac.uk

Exponential asymptotics and problems with coalescing singularities

Philippe H. Trinh and S. Jonathan
Chapman

Oxford Centre for Industrial and Applied Mathematics,
Mathematical Institute, University of Oxford

Problems in exponential asymptotics are typically characterized by divergence of the associated asymptotic expansion in the form of a factorial divided by a power. In this paper, we demonstrate that in certain classes of problems that involve coalescing singularities, a more general type of exponential-over-power divergence must be used. As a model example, we study the water waves produced by flow past an obstruction such as a surface-piercing ship. In the low speed or low Froude limit, the resultant water waves are exponentially small, and their formation is attributed to the singularities in the geometry of the obstruction. However, in cases where the singularities are closely spaced, the usual asymptotic theory fails. We present both a general asymptotic framework for handling such problems of coalescing singularities, and provide numerical and asymptotic results for particular examples.

1. Introduction

Many problems in exponential asymptotics involve the analysis of a singularly perturbed differential equation where the associated solution is expressed as a divergent asymptotic expansion. It has been noted by authors such as [Dingle \[1\]](#) and [Berry \[2\]](#) that in many cases, the divergence of the sequence occurs in the form of a factorial divided by a power. In this paper, we use a model problem from the theory of water waves and ship hydrodynamics to demonstrate how in certain classes of problems, a more general form of divergence must be used in order to perform the exponential asymptotics. This behaviour is expected to occur in a wide range of singular perturbation problems characterized by multiple singularities coalescing in the limit the small parameter tends to zero.

We begin with a brief explanation of exponential asymptotics and factorial-over-power divergence. Consider a re-scaled differential equation for the exponential integral,

$$\epsilon \frac{dy}{dz} + y = \frac{\epsilon}{z}, \quad y \rightarrow 0 \text{ as } z \rightarrow -\infty, \quad (1.1)$$

in the limit $\epsilon \rightarrow 0$, where $y : \mathbb{C} \mapsto \mathbb{C}$, and for which the exact solution is given by $y(z) = e^{-z/\epsilon} \text{Ei}(z/\epsilon)$. Begin by assuming that $\Im(z) < 0$ in (1.1). The usual approach to studying (1.1) is to expand the solution as a series

$$y(z) = \sum_{n=1}^{\infty} \epsilon^n y_n, \quad (1.2)$$

through which it is found that $y_n = (n-1)!/z^n$. However, this approximation remains accurate only when z is in the lower half-plane, $\Im(z) < 0$. If we analytically continue z along a path that crosses the positive real axis, we find that an exponentially small term switches-on across $\Re(z) \geq 0$. This modifies the asymptotic form of (1.2) to

$$y(z) = \sum_{n=1}^{\infty} \epsilon^n y_n + 2\pi i e^{-z/\epsilon}. \quad (1.3)$$

This unusual process is known as the *Stokes Phenomenon* ([Berry \[3\]](#), [Meyer \[4\]](#), [Olde Daalhuis *et al.* \[5\]](#)), and in the case of (1.1), the appearance of the exponentially small terms can be understood through a variety of techniques ranging from studying the integral form of (1.1) and application of the method of steepest descents ([Bleistein & Handelsman \[6\]](#)), to applying Borel transforms ([Dingle \[1\]](#)), optimal truncation ([Chapman *et al.* \[7\]](#)), or series acceleration ([Baker \[8\]](#)).

The key feature in such problems where exponential small terms switch-on or off is the divergence of the naïve asymptotic expansion (1.2). A generic quality of singular problems is that once (1.2) has been truncated at $n = \mathcal{N}$, an equation for the leading-order remainder, $R_{\mathcal{N}}$, will be of the form

$$\mathcal{L}(R_{\mathcal{N}}; \epsilon) \sim \epsilon^{\mathcal{N}} y_{\mathcal{N}}. \quad (1.4)$$

However, in the limit $\epsilon \rightarrow 0$, the optimal truncation point, $\mathcal{N} \rightarrow \infty$, and hence the exponentially small remainder is related to the divergence of the naïve asymptotic expansion. It has been noted, principally by [Dingle \[1\]](#), that in singularly perturbed problems, the divergence of the asymptotic series takes the form

$$y_n \sim \frac{\Gamma(n+a)}{(\text{variable})^n}, \quad (1.5)$$

as $n \rightarrow \infty$, and this ‘factorial-over-power’ divergence of the late terms is understood as the consequence of expanding a function with isolated singularities in the complex plane and also known as Darboux’s Theorem ([Henrici \[9, p.447\]](#)).

In this paper, we demonstrate that for a certain problems that involves coalescing singularities, the divergence of the late terms may take the alternative form of an exponential-over-power,

$$y_n \sim \frac{\Gamma(n+a)!}{(\text{variable})^n} \exp \left[\sum_j (\text{variable}) n^{a_j} \right], \quad (1.6)$$

where $0 < a_j < 1$.

In particular, the theory we describe is applicable for the study of singular nonlinear differential equations of the form

$$\mathfrak{N}(z, y; \epsilon) = F(z, y; a_1(\epsilon), a_2(\epsilon), \dots), \quad (1.7)$$

where \mathfrak{N} is a nonlinear differential operator on $y: \mathbb{C} \mapsto \mathbb{C}$, $z \in \mathbb{C}$, and F is a forcing function that is singular at points $z = -a_k$, in the complex plane. An asymptotic expansion of the solution, y , in the limit $\epsilon \rightarrow 0$ will diverge based on the presence of these singularities, and Stokes lines will necessitate the switching-on of exponentially small terms. However, there exists a distinguished limit whereby the singularities may coalesce (e.g. $a_i \rightarrow a_j$ for distinct i, j), and the study of this distinguished limit is the subject of this paper.

We begin in §2, by presenting a model problem motivated by a previous studies on water waves (Chapman and Vanden-Broeck [10, 11], Trinh and Chapman [12, 13, 14, 15]) on the application of exponential asymptotics to the study of gravity or capillary waves produced by flow over a submerged object. In the limit of low speeds or low Froude numbers, potential flow past an obstruction such as a step in a channel or a surface-piercing ship will produce free surface waves that are exponentially small in the Froude number. These low-Froude water wave problems present a useful setting for studies on exponential asymptotics, as the waves can be directly observed in numerical and experimental settings, and concepts such as Stokes lines and the Stokes Phenomenon share a correspondence with the physical fluid domain.

Then in §3, we review the application of exponential asymptotics to study the case where the singularities are well separated. The techniques we apply are based on the use of a factorial over power ansatz to capture the divergence of the asymptotic expansions, then optimal truncation and Stokes line smoothing to relate the late-order terms to the exponentially small waves (see for example, papers by Olde Daalhuis *et al.* [5], Chapman *et al.* [7], and Trinh [16]). For more details on standard techniques in exponential asymptotics, including other approaches, we refer the reader to the tutorials and reviews by Boyd (1998), Olde Daalhuis [18], Costin [19], and Grimshaw [20].

The problem with coalescing singularities is studied in §4, and we go through the general methodology for a particular case, which is accompanied by numerical verification in §5. A more general methodology is present in Appendix B. Discussion of the results follows in §6.

2. A model for the ship-wave problem

Although the main contents of this paper can be appreciated without understanding the physical context of the differential equations, it is helpful to understand from where the model arose, and the relationship between the mathematical and physical theories.

The governing equations for two-dimensional, steady, incompressible, irrotational, and inviscid flow past a submerged or surface-piercing object in the presence of gravity involves: (i) the solution of Laplace's equation for the fluid potential, ϕ ; (ii) kinematic conditions, on all fluid and solid surfaces; and (iii) a dynamic boundary condition (Bernoulli's equation) for the free surface. In the low speed or low Froude limit, a small non-dimensional parameter, ϵ , representing the balance between inertial and gravitational forces, can be introduced.

We explain in Appendix A that the search for exponentially small free-surface waves in this system can be modeled using the complex initial value problem,

$$\left[\phi - q_s^2 \right] - i\epsilon q_s \phi \frac{d\phi}{dw} = 0, \quad (2.1)$$

with $\phi(0) = 0$, where $w \in \mathbb{R}$, and $\phi: \mathbb{C} \rightarrow \mathbb{C}$. In this paper, we are primarily interested in studying the case where the forcing function, q_s , is given by

$$q_s(w) = \frac{w^{\sigma_1 + \sigma_2}}{(w + a_1)^{\sigma_1}(w + a_2)^{\sigma_2}}, \quad (2.2)$$

where $0 < a_2 < a_1$, $a_1 + a_2 = 1$, and $0 < \sigma_1, \sigma_2 < 1$. We note that in the limit $\epsilon \rightarrow 0$, $\phi \sim q_s$. In terms of the fluid mechanics, this q_s function describes the leading-order low-speed or low-Froude flow past a two-cornered ship with corners located at $w = -a_1$ and $w = -a_2$, and divergent corner-angles $\pi\sigma_1$ and $\pi\sigma_2$.

A numerical solution of the differential equation for $\epsilon = 0.8$ is shown in Figure 1. Here, $a_1 = 0.8$, $a_2 = 0.2$, and $\sigma_1 = \sigma_2 = 1/4$. We note that because of the removable singularity as $w \rightarrow 0$, the numerical solution is solved beginning near $w = 0$ ($w_0 = 10^{-5}$ in the figure) subject to the initial condition of $\phi = q_s^2 + 2\epsilon i q_s^4 q_s'$ evaluated at $w = w_0$ (this expression is derived from the asymptotic expansion as $\epsilon \rightarrow 0$ and is covered later).

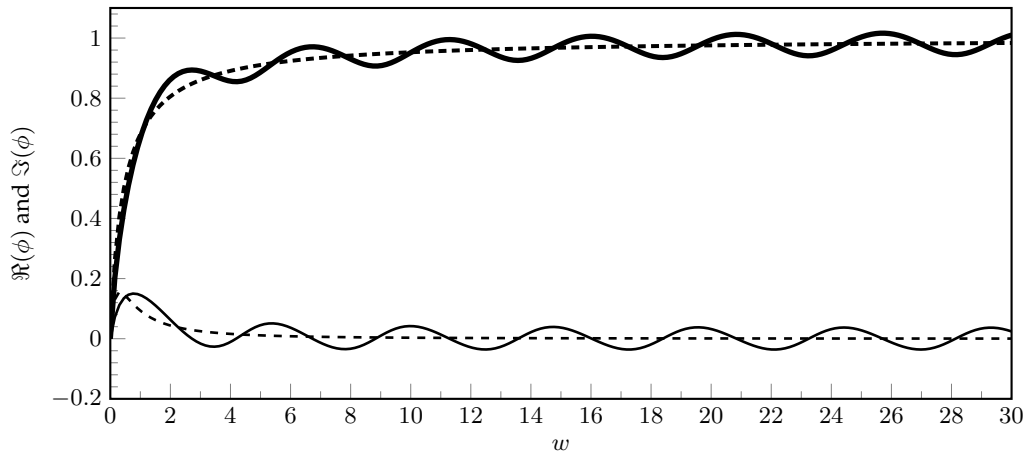


FIGURE 1: Numerical solutions $\Re(\phi)$ (thick) and $\Im(\phi)$ (thin) for $\epsilon = 0.8$, $a_1 = 0.8$, $a_2 = 0.2$, $\sigma_1 = \sigma_2 = 1/4$. The dashed lines correspond to q_s^2 (thick) and $2i q_s^4 q_s'$ (thin).

Our goal in this paper is to derive the form of the waves appearing in Figure 1 for the particular case when the two singularities, a_1 and a_2 , in (2.2) tend to one another as $\epsilon \rightarrow 0$. In the limit that $a_1 \rightarrow a_2 = a$, we intuitively expect that the forcing function can be replaced by the single-singularity forcing,

$$q_s(w) = \left(\frac{w}{w + a} \right)^\sigma, \quad (2.3)$$

with $a > 0$ and $\sigma = \sigma_1 + \sigma_2$. However, as we shall see, the replacement of (2.2) by (2.3) is non-trivial, and several challenging aspects emerge when considering the asymptotic analysis in the distinguished limit of merging singularities.

Although the full problem in (A 1) can be studied using our methods, there are two principle reasons why we prefer to study the differential equation (2.1). The first is that the simplification eases the algebraic complexity of the asymptotic analysis, while still preserving all the features of the theory we wish to present (in relation to the coalescence of singularities).

The second reason is that accurate numerical verification of the asymptotic analysis demands numerical precision of five or six digits of accuracy—otherwise, the fine effects of adjusting the ship's geometry are easily missed; this precision can only be easily achieved for the simpler problem, which does not require the computation of the Cauchy Principal integral of the full governing equations. A similar idea of reducing the boundary integral was used by Tuck [21],

who realized that the integral does not play a significant role in seeking free-surface waves in low-Froude problems.

3. A review of the case of well-separated singularities

The theory for the nonlinear equations of low-speed ship flows with well-separated singularities was presented in [13]. Here, although we study a slightly different problem (2.1), we shall only review the main procedure for applying exponential asymptotics, with particular emphasis on the breakdown when the singularities are closely spaced.

(a) Step 1: Characterize divergence of late terms

We begin as usual by applying a regular asymptotic expansion to (2.1)

$$\phi = \sum_{n=0}^{\infty} \epsilon^n \phi_n, \quad (3.1)$$

valid in the limit $\epsilon \rightarrow 0$. The leading-order solution is the rigid-wall flow of (??),

$$\phi_0 = q_s^2 = \left(\frac{w^{\sigma_1 + \sigma_2}}{(w + a_1)^{\sigma_1} (w + a_2)^{\sigma_2}} \right)^2, \quad (3.2)$$

and we note the presence of singularities at $w = -a_1$ and $w = -a_2$, which are related to the physical corners of the ship. At $\mathcal{O}(\epsilon^n)$, we obtain

$$\phi_n = i\epsilon q_s \left[\left(\phi_0 \phi'_{n-1} + \phi_1 \phi'_{n-2} + \dots \right) + \left(\phi_{n-1} \phi'_0 + \dots \right) \right]. \quad (3.3)$$

The calculation of ϕ_n at each order relies upon the differentiation of ϕ_{n-1} , and thus at each order of the asymptotic procedure, we increase the power of the singular term from the previous order. In the limit $n \rightarrow \infty$, the late terms diverge as a factorial over power of the form,

$$\phi_n \sim \frac{P_1(w) \Gamma(n + \gamma_1)}{[\chi_1(w)]^{n + \gamma_1}} + \frac{P_2(w) \Gamma(n + \gamma_2)}{[\chi_2(w)]^{n + \gamma_2}}. \quad (3.4)$$

where $\chi = \chi_k$ are known as the *singulants*, and $\chi_1(-a_1) = 0 = \chi_2(-a_2)$ from the two singularities in the leading-order equation (3.2). Once the ansatz (3.4) is substituted into (3.3), we obtain from the leading-order contribution as $n \rightarrow \infty$ the expressions for χ_1 and χ_2 , given by

$$\chi_k(w) = \int_{-a_k}^w \frac{i}{q_s^3(\varphi)} d\varphi. \quad (3.5)$$

Using the expression of χ_k , Stokes lines can be traced from each of the two singularities, across which the Stokes Phenomenon necessitates the switching-on of waves. From Dingle [1], these special lines are given at the points, $w \in \mathbb{C}$, where

$$\Im[\chi_k(w)] = 0 \quad \text{and} \quad \Re[\chi_k(w)] \geq 0. \quad (3.6)$$

The Stokes lines are numerically computed by integrating (3.5) and are shown in Figure 2 for a particular case. We observe Stokes lines emerging from $w = -a_1$ and $w = -a_2$, curve into the upper half- w -plane, and the intersect the positive real w -axis. It is expected that across these two points of intersection, an exponential switches on. Also shown (dashed) in the figure is the Stokes line that corresponds to the one-singularity function (2.3).

At the subsequent order in (3.3) as $n \rightarrow \infty$, using the ansatz (3.4), we obtain

$$P_k(w) = \frac{\Lambda_k}{q_s^4(w)}, \quad (3.7)$$

where Λ_k is a constant prefactor that must be calculated from matching the outer asymptotic expansion (3.1) with the nonlinear solution near the singularities, $w = -a_k$. Finally, the value of

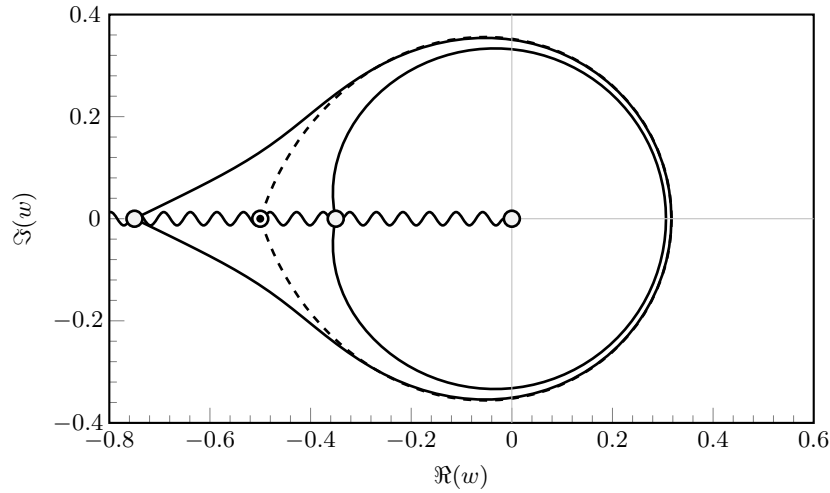


FIGURE 2: (Solid) Stokes lines for (2.2) for $a_1 = 0.75$, $a_2 = 0.35$ and $\sigma_1 = \sigma_2 = 1/4$. (Dashed) Stokes line for (2.3) for $a = 0.5$ and $\sigma = 1/2$. The branch cuts for each of the critical points in q_s is taken along the negative real axis and shown as a snaking curve.

γ_k can be derived by requiring the singular behaviour of ϕ_n in (3.4) to match ϕ_0 when $n = 0$. This gives a value of

$$\gamma_k = \frac{6\sigma_k}{1 + 3\sigma_k}. \quad (3.8)$$

(b) Step 2: Match with the solution near the singularity

In order to determine the unknown pre-factors Λ_k that characterize the divergence of the late terms in (3.4), we must rescale w and ϕ near the singularities, $w = -a_k$, and match to the outer solution found in the previous section. The size of this inner region can be derived by observing where the breakdown in the outer expansion (3.1) first occurs, *i.e.* where $\epsilon q_1 \sim q_0$. We obtain the scaling of ϕ from (3.2) and then this inner region is delimited by

$$\phi = \mathcal{O}(q_s^2) = \mathcal{O}\left((w + a_k)^{-2\sigma_k}\right) \quad \text{and} \quad w + a_k \sim \mathcal{O}\left(\epsilon^{\frac{1}{1+3\sigma_k}}\right). \quad (3.9)$$

Once ϕ and w have been rescaled with (3.9) in mind, then a recurrence relation can be developed for the inner solution, which is then numerically solved (if required), then required to match with (3.1) in order to determine Λ_k . To be specific, we note that as $w \rightarrow -a_k$,

$$q_s \sim c_k (w + a_k)^{-\sigma_k}, \quad (3.10)$$

where the complex constant c_k is computed from (2.2). Within the inner region, the solution, ϕ , can be expanded as an infinite series

$$\phi = c^2 (w + a_k)^{-2\sigma_k} \sum_{n=0}^{\infty} \frac{A_n}{z^n}, \quad (3.11)$$

where $z = X(w + a_k)^{1+3\sigma_k}/\epsilon$, where $X = i/[c^3(1 + 3\sigma_k)]$. We then find that the coefficients, A_n , are found by solving

$$A_0 = 1, \quad A_n = \sum_{m=0}^{n-1} \left(m + \frac{2\sigma_k}{1 + 3\sigma_k} \right) \phi_m \phi_{n-m-1}, \quad \text{for } n > 1. \quad (3.12)$$

As $n \rightarrow \infty$, the divergence of the A_n coefficients is anticipated by the constant, $\Omega(\sigma_k) = A_n/\Gamma(n + \gamma_k)$, which can be computed numerically. Finally, matching the outer series (3.1) with the inner

series (3.11) gives a value for the unknown prefactor,

$$\Lambda_k = \frac{c_k^{6-3\gamma_k} e^{\frac{\pi i}{2} \gamma_k}}{(1+3\sigma_k)^{\gamma_k}} \Omega(\sigma_k). \quad (3.13)$$

This completes the determination of all components of the late terms, ϕ_n , in (3.4).

(c) Step 3: Optimally truncate and smooth the Stokes line

To derive the form of the exponentials that appear whenever a Stokes Line intersects the free-surface, we optimally truncate the asymptotic expansions (3.1), and examine the remainder as the Stokes line is crossed. We let:

$$\phi = \sum_{n=0}^{\mathcal{N}-1} \epsilon^n \phi_n + R_{\mathcal{N}}, \quad (3.14)$$

When \mathcal{N} is chosen to be the optimal truncation point, the remainder $R_{\mathcal{N}}$ is found to be exponentially small, and by re-scaling near the Stokes line, it can be shown that a wave of the following form switches on:

$$\phi_{\text{exp}, k} \sim -\frac{2\pi i}{\epsilon^{\gamma_k}} P_k \exp\left[-\frac{\chi_k}{\epsilon}\right]. \quad (3.15)$$

where $k = 1, 2$, and note that such a contribution is only included if the associated Stokes line from $w = -a_k$ intersects the positive real w -axis (the negative sign is due to a switching moving in the direction of positive w across the Stokes line).

Since $P_k = \Lambda_k/q_0^A(w) \rightarrow \Lambda_k$ as $w \rightarrow \infty$ by (3.7), then the form of the far-field waves are

$$\Re(\phi_{\text{exp}, k}) \sim -\frac{2\pi \Omega(\sigma_k)}{\epsilon^{\gamma_k}} \left[\frac{|c_k|^{6-3\gamma_k}}{(1+3\sigma_k)^{\gamma_k}} \right] \exp\left[-\frac{\Re(\chi_k)}{\epsilon}\right] \sin\left(-\frac{w}{\epsilon} + \Psi_k\right) \quad (3.16)$$

where the phase shift is

$$\Psi_k = -\frac{1}{\epsilon} \Im \left[\int_{-a_k}^{-a_1} \frac{d\chi}{d\varphi} d\varphi \right] + (6-3\gamma_k) \text{Arg}(c_k) + \frac{\pi}{2} \gamma_k. \quad (3.17)$$

We also note that if we use a single-singularity function for q_s in the differential equation (2.1) given by (2.3), then the same exponentially small prediction (3.16) applies with $\chi_k = \chi = \int i/q_s^2 d\varphi$ as in (3.5). The key to note is that within the outer region, where the ansatz (3.4) plays an important role, the precise nature of the q_s function is unimportant. The determination of the prefactor P_k in the ansatz requires matching with an inner solution, where $q_s \sim c_k(w+a_k)^{-\sigma_k}$; since the single-singularity q_s in (2.3) contains the same local behaviour, the exponential prediction (3.16) follows identically with $c = c_k$, $\sigma = \sigma_k$, and so on.

The requirement for a distinguished limit for merging singularities can be observed by computing numerical solutions of (2.1) with a fixed values of ϵ and σ_1, σ_2 , but allowing the singularities to approach one another. The wave amplitude for such a computation is shown in Figure 3 in the case of the two-singularity forcing (2.2). We see that the asymptotic prediction (3.16) is accurate when the singularities are well separated, but diverges once the singularities approach one another. A uniform approximation would need to smoothly match with the one-singularity approximation at one end, and the (separated) two-singularity analysis at the other.

4. Two closely spaced singularities with $\sigma = 1/3$

From the well-separated analysis of §3, we observed that when the inner region corresponding to the singularities is of the size $\mathcal{O}(\epsilon^{1/(1+3\sigma_k)})$, and thus as $a_2 \rightarrow a_1$, the singularities coalesce and the previous asymptotic methodology breaks down.

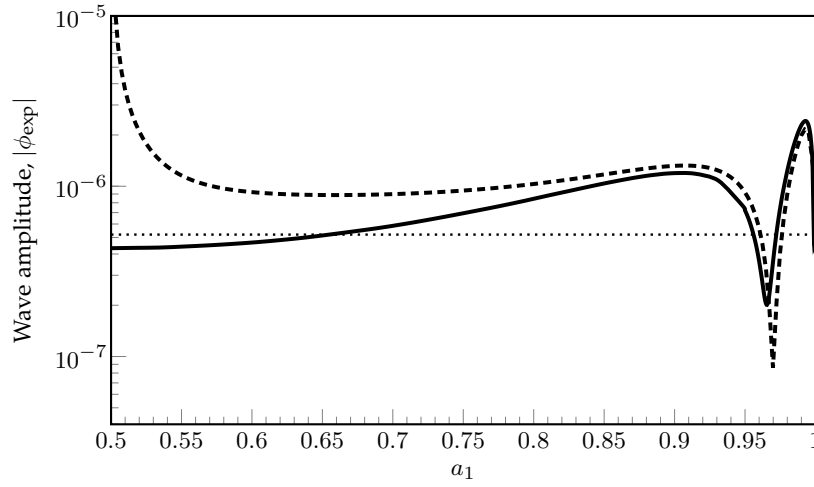


FIGURE 3: The numerical solution (solid) for the $\sigma_1 = \sigma_2 = 1/4$ forcing is plotted against the well-separated asymptotic approximation at $\epsilon = 0.15$ and $a_1 + a_2 = 1$ (dashed). The two-singularity approximation very accurately predicts the solution when the two singularities are well spaced, but is singular when $a_1, a_2 \approx 0.5$ near the left. The dotted line indicates the one-singularity approximation for $\sigma = 1/3$ and $a = 0.5$.

We shall study a problem where the singularities are located a distance $\epsilon^{\ell/m}\beta$ on either side of $w = -a$ (with $a, \beta > 0$). The positive integers ℓ and m are defined such that

$$\frac{\ell}{m} \equiv \frac{1}{1 + 3\sigma} \quad (4.1)$$

where $\sigma = \sigma_1 + \sigma_2$ and the ratio ℓ/m is irreducible. Now from (2.2), we obtain the geometry (for the ship), given by

$$q_s = \frac{w^\sigma}{(w + a + \epsilon^{\ell/m}\beta)^{\sigma_1}(w + a - \epsilon^{\ell/m}\beta)^{\sigma_2}}, \quad (4.2)$$

or, as an expansion in ϵ ,

$$q_s = \left(\frac{w}{w + a}\right)^\sigma \sum_{n=0}^{\infty} \epsilon^{\frac{\ell n}{m}} \left(\frac{\beta}{w + a}\right)^n f_n, \quad (4.3)$$

where $f_0 = 1$, $f_1 = \sigma_2 - \sigma_1$, $f_2 = \frac{1}{2}[(\sigma_1 - \sigma_2)^2 + \sigma_1 + \sigma_2]$, and in general,

$$f_n = \frac{1}{\Gamma(\sigma_1)\Gamma(\sigma_2)} \sum_{m=0}^n (-1)^m \frac{\Gamma(\sigma_1 + m)\Gamma(\sigma_2 + n - m)}{\Gamma(m + 1)\Gamma(n - m + 1)}. \quad (4.4)$$

Note that the governing equation (2.1) naturally leads to an expansion in powers of ϵ , but the fact that q_s is a series in $\epsilon^{\ell/m}$ forces us to expand ϕ in the more finely spaced powers of $\epsilon^{1/m}$. Our approach, then, is only applicable for cases where σ_1 and σ_2 are rational; this is a key requirement in order for the expansions of ϕ and q_s to ‘interleave’ properly. Irrational angles will require more general asymptotic expansions and is beyond the scope of this work.

Although it is a straightforward to extend the methodology to handle general rational values of σ_1 and σ_2 , we will begin by studying the particular case of geometry for which $\sigma_1 + \sigma_2 = 1/3$ for the geometry q_s in (4.3). The general methodology is presented in the Appendix.

Setting $\ell = 1$ and $m = 2$ in (4.1). From (4.2) and (4.3) we have

$$q_s(w) = \frac{w^{1/3}}{(w+a+\sqrt{\epsilon\beta})^{\sigma_1}(w+a-\sqrt{\epsilon\beta})^{\sigma_2}} = q_0 \sum_{n=0}^{\infty} \epsilon^{\frac{n}{2}} e_n, \quad (4.5)$$

with $q_0 = [w/(w+a)]^\sigma$ and where we have defined

$$e_n = \left(\frac{\beta}{w+a} \right)^n f_n, \quad (4.6)$$

with f_n as in (4.4).

(a) Outer analysis and exponential-over-power ansatz

We substitute the naive asymptotic expansion,

$$\phi = \sum_{n=0}^{\infty} \epsilon^{1/2} \phi_n, \quad (4.7)$$

into (2.1), giving for the low-order terms

$$\phi_0 = q_0^2 = \left(\frac{w}{w+a} \right)^{2/3}, \quad (4.8a)$$

$$\phi_1 = q_0^2 \sum_{k=0}^1 e_k e_{1-k}, \quad (4.8b)$$

$$\phi_2 = q_0^2 \sum_{k=0}^2 e_k e_{2-k} + 2ie_0 q_0^4 \frac{dq_0}{dw}. \quad (4.8c)$$

The general equation at $\mathcal{O}(\epsilon^{n/2})$ is unwieldy, but we shall seek only those terms that are needed to describe the $n \rightarrow \infty$ behaviour. The relevant terms are given by

$$\begin{aligned} 1 - iq_0 \left[e_0 \phi_0 \right] \frac{\phi'_{n-2}}{\phi_n} - iq_0 \left[e_0 \phi_1 + e_1 \phi_0 \right] \frac{\phi'_{n-3}}{\phi_n} \\ - iq_0 \left[e_0 \phi_2 + e_1 \phi_1 + e_2 \phi_0 \right] \frac{\phi'_{n-4}}{\phi_n} - iq_0 \left[e_0 \phi'_0 \right] \frac{\phi_{n-2}}{\phi_n} + \dots = 0, \end{aligned} \quad (4.9)$$

where we have divided the $\mathcal{O}(\epsilon^{n/2})$ by ϕ_n to ease the expansions to follow. Like in §3(a), the merged singularity at $w = -a$ in (4.8a) will cause the late terms to diverge. However, if we substitute the usual factorial-over-power ansatz into (4.9) we discover terms of order $1/\sqrt{n}$ are created, which cannot be matched. In fact, for the divergence of the close-singularities problem, the correct late-order behaviour is described by a more general exponential-over-power ansatz of the form

$$\phi_n \sim \frac{P(w) \Gamma\left(\frac{n}{2} + \gamma\right) \exp[r_1(w)\sqrt{n}]}{[\chi(w)]^{\frac{n}{2} + \gamma}}, \quad (4.10)$$

valid in the limit $n \rightarrow \infty$. The *singulant* function, $\chi(w)$, will be solved subject to the requirement that $\chi(-a) = 0$. Note that instead of the factorial in (4.10), we could use the alternative expression

$$\phi_n = \frac{\tilde{P}(w)}{[\chi(w)]^{n/2 + \gamma(w)}} \exp \left[\frac{n}{2} \log n + b(w)n + c(w)\sqrt{n} + d(w) \log n \right]. \quad (4.11)$$

If we do this, then we would find that $b(w) = -1/2(1 + \log 2)$ is the simplest choice (can be absorbed into χ), and $d(w) = \gamma - 1/2$ is another convenient choice, where $\gamma(w) = \gamma$ is constant. The difference between these two ansatzes is only a numerical prefactor, with $\tilde{P}_k = \sqrt{2\pi} 2^{-(\gamma-1/2)} P$. We prefer to preserve the connection to the Gamma function so opt for (4.10).

Substituting this ansatz into (4.9) and expanding the ratios gives

$$\begin{aligned} 1 - iq_0 \left[e_0 \phi_0 \right] & \left\{ -\chi' + \frac{\chi' r_1 + 2\chi r_1'}{\sqrt{n}} + \left(\frac{4\chi P' - \chi' P r_1^2 - 4\chi P r_1 r_1'}{2P} \right) \frac{1}{n} + \mathcal{O}\left(\frac{1}{n^{\frac{3}{2}}}\right) \right\} \\ & - iq_0 \left[e_0 \phi_1 + e_1 \phi_0 \right] \left\{ -\frac{\sqrt{2}\chi\chi'}{\sqrt{n}} + \left(\frac{3\sqrt{\chi}\chi' r_1}{\sqrt{2}} + 2\sqrt{2}\chi^{3/2} r_1' \right) \frac{1}{n} + \mathcal{O}\left(\frac{1}{n^{\frac{3}{2}}}\right) \right\} \\ & - iq_0 \left[e_0 \phi_2 + e_1 \phi_1 + e_2 \phi_0 \right] \left\{ -\frac{2\chi\chi'}{n} + \mathcal{O}\left(\frac{1}{n^{\frac{3}{2}}}\right) \right\} - iq_0 \left[e_0 \phi_0' \right] \left\{ \frac{2\chi}{n} + \mathcal{O}\left(\frac{1}{n^{\frac{3}{2}}}\right) \right\} = 0. \end{aligned} \quad (4.12)$$

Once we substitute the early orders (4.8) into the $\mathcal{O}(\epsilon^{n/2})$ equation (4.12) and take the $n \rightarrow \infty$ limit, we obtain at $\mathcal{O}(1)$, $\mathcal{O}(1/n)$, and $\mathcal{O}(1/\sqrt{n})$ three differential equations for the component functions of the late-order ansatz (4.10). These are given by

$$\frac{d\chi}{dw} = \frac{i}{q_0^3}, \quad (4.13a)$$

$$\frac{dr_1}{dw} = \frac{3ie_1}{\sqrt{2}\chi q_0^3} - \frac{ir_1}{2\chi q_0^3}, \quad (4.13b)$$

$$\frac{1}{P} \frac{dP}{dw} = -\frac{4q_0'}{q_0} + \frac{i}{q_0^3} \left(-6e_1^2 + 3ie_2 + \frac{3e_1 r_1}{2\sqrt{2}\chi} - \frac{r_1^2}{4\chi} \right). \quad (4.13c)$$

We substitute the value of q_0 in (4.8a) into (4.13a), and solve for the singular function subject to $\chi(-a) = 0$, giving

$$\chi(w) = i \left[(w+a) + a \log w - a \log(-a) \right] = a\pi + i \left[(w+a) + a \log(w/a) \right]. \quad (4.14)$$

Here, we will select the principal branch of the logarithm in order for $\Re(\chi) > 0$ when $w > 0$ (ensuring that the exponentials that are switched-on in §4(d) decay as $\epsilon \rightarrow 0$). We can then use χ in (4.14) to solve the equation for r_1 in (4.13b), giving

$$r_1(w) = \frac{3}{\sqrt{2}\chi} \left[\int_{-a}^w \frac{d\chi}{d\varphi} e_1(\varphi) d\varphi + \text{const.} \right] = \frac{3i\beta f_1}{\sqrt{2}\chi} \log(-w/a), \quad (4.15)$$

where e_1 follows from (4.6) and the constant of integration chosen with the requirement that $r_1(w)$ is bounded as $w \rightarrow -a$. We note that it can be difficult to see which logarithmic and square root branch of (4.15) must be used. We shall leave these choices ambiguous for now, but it will become clear which branches must be selected in the next section.

Turning to (4.13c), we can use the preceding differential equations for χ and r_1 , and the expressions for e_1 and e_2 in (4.6) to integrate the right hand-side explicitly, giving

$$P = \Delta \left[q_0(w) \right]^{-4-3iA} \exp \left[\frac{r_1^2(w)}{4} \right], \quad (4.16)$$

for some complex-valued constant Δ and $A = 3\beta^2(2f_1^2 - f_2)/a$.

The value of γ in the late-order ansatz (4.10) can be derived by requiring that the behaviour of the ansatz at $n=0$ matches the behaviour of q_0 in (4.8a) as the singularity is approached. As $w \rightarrow -a$, we see using (4.18) that $\phi_n = \mathcal{O}(w+a)^{4/3+iA-2\gamma}$ must match $q_0^2 = \mathcal{O}(w+a)^{-2/3}$. Solving for γ , we obtain

$$\gamma = \gamma_r + i\gamma_c, \quad \text{where } \gamma_r = 1, \gamma_c = \frac{3\beta^2}{2a}(2f_1^2 - f_2). \quad (4.17)$$

We have the following behaviours as the $w \rightarrow -a$:

$$q_0 \sim c(w + a)^{1/3}, \quad \text{where } c = (-a)^{1/3} \quad (4.18a)$$

$$\chi \sim X(w + a)^2, \quad \text{where } X = -i/2a \quad (4.18b)$$

$$r_1 \sim \mu_1, \quad \text{where } \mu_1 = 3\sqrt{2X}\beta f_1 \quad (4.18c)$$

$$P \sim \Delta \left[c(w + a)^{-\frac{1}{3}} \right]^{2(1-3\gamma)} e^{\mu_1^2/4}, \quad \text{where } \gamma = 1 + i(3\beta^2/a)(2f_1^2 - f_2). \quad (4.18d)$$

This completes our derivation of the form of the late terms (4.10) of the asymptotic expansion. In §4(d), we shall discover a connection between the exponentials switched-on due to the Stokes Phenomenon and these late terms. However, the value of Δ in (3.7) is still unknown, and is obtained by matching the inner and outer expansions.

(b) Inner analysis near the singularity

The inner region occurs near $w = -a$ when $\sqrt{\epsilon}\phi_1 \sim \phi_0$ and the asymptotic expansion (4.7) begins to rearrange. Using the leading-order scaling of $\phi \sim q_0^2$, we introduce inner variables, z and $\hat{\phi}$, defined by

$$w + a = (\epsilon/X)^{1/2} z \quad \text{and} \quad \phi = c^2(w + a)^{-2/3} \hat{\phi}. \quad (4.19)$$

where c and X are from (4.18a) and (4.18b). We also write $q_s(w) = q_0 \hat{q}_s$, and from (4.5),

$$\hat{q}_s = \sum_{n=0}^{\infty} \frac{\beta^n X^{n/2} f_n}{z^n} \equiv \sum_{n=0}^{\infty} \frac{\hat{e}_n}{z^n}. \quad (4.20)$$

Using the scalings (4.19) in (2.1), we obtain the leading-order inner equation is given by

$$\frac{1}{2z^2} \left[-\frac{2}{3} \hat{q}_s \hat{\phi}^2 + z \hat{q}_s \hat{\phi} \frac{d\hat{\phi}}{dz} \right] + [\hat{\phi} - \hat{q}_s^2] = 0. \quad (4.21)$$

We wish to study the leading-order solution, $\hat{\phi}$, as it tends outwards towards the outer region. Within the limit $z \rightarrow \infty$, we expand

$$\hat{\phi} = \sum_{n=0}^{\infty} \frac{A_n}{z^n}, \quad (4.22)$$

and substitute this series into the inner equation (4.21), giving the recurrence relations

$$A_0 = 1, \quad A_1 = \sum_{j=0}^1 \hat{e}_j \hat{e}_{1-j} \quad (4.23a)$$

$$A_n = \sum_{j=0}^n \hat{e}_j \hat{e}_{n-j} + \sum_{k=0}^{n-2} \hat{e}_k \left[\sum_{j=0}^{n-2-k} \left(\frac{j+2/3}{2} \right) A_j A_{n-2-k-j} \right] \quad \text{for } n > 1. \quad (4.23b)$$

A simple numerical computation assures us that A_n diverges in the limit $n \rightarrow \infty$. As in the outer analysis of the previous section, a standard factorial divergence is insufficient, an additional exponential growth in n accompanies A_n . We posit that in the limit $n \rightarrow \infty$, the divergence of A_n is captured by the two possible ansatzes

$$A_n \sim \Omega^{\text{cc}} e^{i\tau} \Gamma\left(\frac{n}{2} + \gamma\right) \exp\left[\mu_1 \sqrt{n}\right] \quad (4.24a)$$

or

$$A_n \sim (-1)^n \Omega^{\text{cc}} e^{i\tau} \Gamma\left(\frac{n}{2} + \gamma\right) \exp\left[\mu_1 \sqrt{n}\right], \quad (4.24b)$$

where γ and μ_1 are real constants to be determined (and will be found to be identical to the same constants as defined in the outer analysis of the previous section). Notice that changing the square-root branch of (4.20) produces a factor of $(-1)^n$ in the expansion of \hat{q}_s . We will proceed with the assumption that (4.24a) is correct, and demonstrate how this choice affects the analysis.

The remaining Ω^{cc} and τ are real constants to be determined. Once (4.24a) is substituted into the recurrence relation for A_n in (A 4b), the relevant terms are found to be

$$1 - \left[\frac{\hat{e}_0 A_0}{2} \right] \frac{n A_{n-2}}{A_n} - \left[\frac{\hat{e}_0 A_1 + \hat{e}_1 A_0}{2} \right] \frac{n A_{n-3}}{A_n} - \left[\frac{\hat{e}_0 A_2 + \hat{e}_1 A_1 + \hat{e}_2 A_0}{2} \right] \frac{n A_{n-4}}{A_n} + \left[\frac{\hat{e}_0 A_0}{3} \right] \frac{A_{n-2}}{A_n} + \dots = 0, \quad (4.25)$$

and expanding the ratios of A_n gives

$$1 - \left[\frac{\hat{e}_0 A_0}{2} \right] \left\{ 2 - \frac{2\mu_1}{\sqrt{n}} + \frac{4 - 4\gamma + \mu_1^2}{n} + \mathcal{O}\left(\frac{1}{n^{3/2}}\right) \right\} - \left[\frac{\hat{e}_0 A_1 + \hat{e}_1 A_0}{2} \right] \left\{ \frac{2\sqrt{2}}{\sqrt{n}} - \frac{3\sqrt{2}\mu_1}{n} + \mathcal{O}\left(\frac{1}{n^{3/2}}\right) \right\} - \left[\frac{\hat{e}_0 A_2 + \hat{e}_1 A_1 + \hat{e}_2 A_0}{2} \right] \left\{ \frac{4}{n} + \mathcal{O}\left(\frac{1}{n^{3/2}}\right) \right\} + \left[\frac{\hat{e}_0 A_0}{3} \right] \left\{ \frac{2}{n} + \mathcal{O}\left(\frac{1}{n^{3/2}}\right) \right\} = 0. \quad (4.26)$$

Setting $\hat{e}_0 = A_0 = 1$, then (4.26) is satisfied identically at $\mathcal{O}(1)$. Afterwards, the $\mathcal{O}(1/\sqrt{n})$ and $\mathcal{O}(1/n)$ terms give

$$\mu_1 = 3\sqrt{2}\hat{e}_1 = 3\sqrt{2X}\beta f_1, \quad (4.27a)$$

$$\gamma = 1 - 6\hat{e}_1^2 + 3\hat{e}_2 = 1 - 3\beta^2 X [2f_1^2 - f_2]. \quad (4.27b)$$

where we have set $\hat{e}_1 = \beta\sqrt{X}f_1$ and $\hat{e}_2 = \beta^2 X f_2$. In fact, this independently verifies the inner limit of $r_1(w) \rightarrow \mu_1$ obtained in the outer analysis in (4.18c), as well as the γ constant in (4.17).

Now that the exponential growth of the divergent ansatz of A_n in (4.24a) has been fully determined, the values of Ω^{cc} and τ can be computed by numerically solving the full nonlinear recurrence relation (4.23) and using

$$H_n \equiv \frac{A_n}{\Gamma(\frac{n}{2} + \gamma)e^{\mu_1\sqrt{n}}} \rightarrow \Omega^{\text{cc}} e^{i\tau} \quad (4.28)$$

in the limit $n \rightarrow \infty$.

In Figure 4, we plot H_n for the two cases $\sigma_1 = 3/24$, $\sigma_2 = 5/24$ (a) and $\sigma_1 = 6/24$, $\sigma_2 = 2/24$ (b). The remaining parameters are set to $a = 1$ and $\beta = 1$. The convergence towards the constant values in each of the graphs is algebraic in n , and confirms that the exponential growth was correctly predicted. For both the values of $|H_n|$ and $\text{Arg}(H_n)$, the values can be seen to alternate between two branches—this is effectively a consequence of the $\sqrt{\epsilon}$ series in q_s . For other ℓ/m values in (4.1), it can be expected that m branches of the recurrence relation would be observed for most cases of σ_1 and σ_2 (See Appendix B for discussion of the methodology for more general singularities).

Now had we used (4.24b) with the extra factor of $(-1)^n$, we would note that the value of γ in (4.27b) remains the same, but the value of μ_1 in (4.27a) changes to $-3\sqrt{2}\hat{e}_1$. Both forms of (4.24) are possible, but one contribution will exponentially dominate the other. The proper choice of ansatz can be determined based on the fact we need $\Re(\mu_1) > 0$ in order to describe the divergent A_n values in (4.28). Since $f_1 = \sigma_2 - \sigma_1$ in (4.4) and $\beta > 0$, we define

$$\mu_1 = 3\beta|\sigma_2 - \sigma_1|\sqrt{2|X|}e^{-\pi i/4}, \quad (4.29)$$

which ensures that $\Re(\mu_1) > 0$ regardless of the sign of $(\sigma_2 - \sigma_1)$. Indeed, without taking care to choose the correct ansatz, the graphs of $|H_n|$ in Figure 4 would display exponential growth (due to underpredicting the divergence) or the points in the graphs of $\text{Arg}(H_n)$ may alternate by $\pm\pi$.

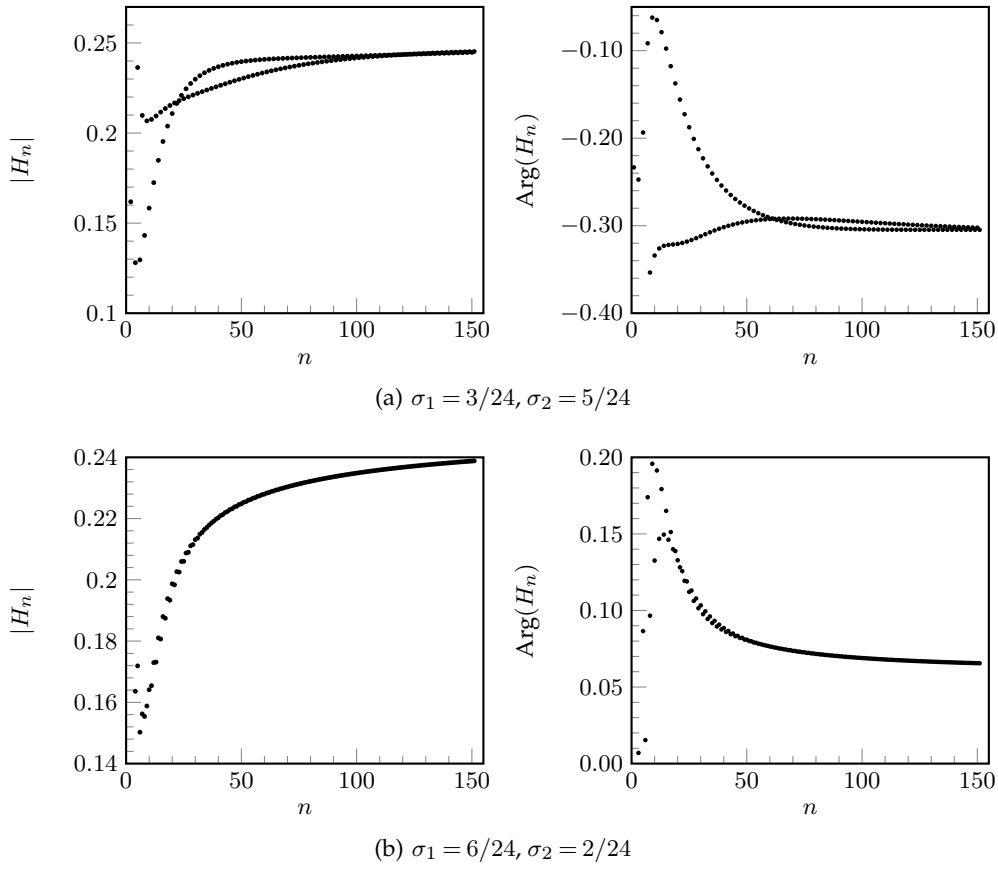


FIGURE 4: Magnitude and phase of $H_n = A_n / [\Gamma(n/2 + \gamma)e^{\mu_1\sqrt{n}}]$, representing the solutions of the recurrence relation (4.23) once the exponential growth has been scaled out. Two different σ_1 and σ_2 pairs are used, and $a = 1, \beta = 1$ for both.

(c) Matching inner and outer ansatzes

By Van Dyke's matching rule [22], the n^{th} term of the outer expansion ($n.t.o$) given by the ansatz (4.10), written in inner coordinates, and keeping the first term (1.t.i) yields

$$\phi \xrightarrow{(n.t.o)} \epsilon^{\frac{n}{2}} \phi_n \sim \frac{P\Gamma(\frac{n}{2} + \gamma)e^{r_1 n^{1/2}}}{\chi^{\frac{n}{2} + \gamma}} \xrightarrow{(1.t.i)} \frac{\Delta c^{2(1-3\gamma)} W^{-2\sigma} e^{\mu_1^2/4} \Gamma(\frac{n}{2} + \gamma) e^{\mu_1 n^{1/2}}}{X^\gamma z^n}, \quad (4.30)$$

where we have used the inner limits of χ , r_1 , and P in (4.18). This expression provides a match with the first term of the inner approximation (1.t.i) given by (4.22), written in outer variables and re-expanded to n terms ($n.t.o$),

$$\phi = c^2 W^{-2\sigma} \hat{\phi} \xrightarrow{(1.t.i)} c^2 W^{-2\sigma} \sum_{n=0}^{\infty} \frac{A_n}{z^n} \xrightarrow{(n.t.o)} c^2 W^{-2\sigma} \frac{[\Omega^{\text{cc}} e^{i\tau}] \Gamma(\frac{n}{2} + \gamma) e^{\mu_1 \sqrt{n}}}{z^n}. \quad (4.31)$$

Matching then allows us to obtain the value of outer prefactor, Δ , as a function of the inner pre-factors $\Omega^{\text{cc}} e^{i\tau}$, and thus $\Delta = c^{6\gamma} X^\gamma e^{-\mu_1^2/4} [\Omega^{\text{cc}} e^{i\tau}]$. In summary, P is given by

$$P(w) = (c^6 X)^\gamma [\Omega^{\text{cc}} e^{i\tau}] [q_0(w)]^{2(1-3\gamma)} \exp\left[\frac{1}{4}(r_1^2(w) - \mu_1^2)\right]. \quad (4.32)$$

We have thus obtained all the components of the late-order ansatz for ϕ_n in (4.10). It remains to relate these late terms to the exponential switching.

(d) Optimal truncation and Stokes line smoothing

We now truncate the asymptotic expansion of ϕ in (4.7) at $n = \mathcal{N}$,

$$\phi = \sum_{n=0}^{\mathcal{N}-1} \epsilon^{n/2} \phi_n + R_{\mathcal{N}}, \quad (4.33)$$

and substitute this equation into the differential equation for ϕ in (2.1). This yields an equation of the form

$$\mathcal{L}(R_{\mathcal{N}}; \epsilon) \sim \epsilon^{\mathcal{N}/2} \phi_{\mathcal{N}}, \quad (4.34a)$$

with \mathcal{L} given by

$$\begin{aligned} \mathcal{L}(R_{\mathcal{N}}; \epsilon) \equiv & R_{\mathcal{N}} - iq_0 [e_0 \phi_0] \epsilon R'_{\mathcal{N}} - iq_0 [e_0 \phi_1 + e_1 \phi_0] \epsilon^{3/2} R'_{\mathcal{N}} \\ & - iq_0 [e_0 \phi_2 + e_1 \phi_1 + e_2 \phi_0] \epsilon^2 R'_{\mathcal{N}} - iq_0 [e_0 \phi'_0] \epsilon R_{\mathcal{N}} + \dots \end{aligned} \quad (4.34b)$$

Our goal in this section is to choose $n = \mathcal{N}$ optimally, so that the remainder is exponentially small. In the limit that $\epsilon \rightarrow 0$, $\mathcal{N} \rightarrow \infty$, and the inhomogeneous differential equation for the remainder (4.34a) will be forced by the exponential-over-power ansatz of (4.10). We shall find that as the Stokes line, $\Im(\chi) = 0$ and $\Re(\chi) \geq 0$, is crossed the exponentially small remainder switches on. The distinction of our work here, compared to the previous studies of, *e.g.* Chapman *et al.* [7], is that the exponential-over-power ansatz modifies the connection between $\phi_{\mathcal{N}}$ and $R_{\mathcal{N}}$. Effectively, the Stokes line is shifted in location due to the multiple singularities.

To begin, we express the solution of the homogeneous equation, $\mathcal{L} = 0$, in (4.34), by setting

$$R_{\mathcal{N}} = \overline{P}(w) e^{F(w)} = \overline{P}(w) \exp \left[\frac{F_0(w)}{\epsilon} + \frac{F_1(w)}{\sqrt{\epsilon}} \right], \quad (4.35)$$

into (4.34b) and dividing by $R_{\mathcal{N}}$, giving

$$\begin{aligned} 1 - iq_0 [e_0 \phi_0] \left[F'_0 + \sqrt{\epsilon} F'_1 + \epsilon \frac{\overline{P}'}{\overline{P}} \right] - iq_0 [e_0 \phi_1 + e_1 \phi_0] \left[\sqrt{\epsilon} F'_0 + \epsilon F'_1 + \mathcal{O}(\epsilon^{\frac{3}{2}}) \right] \\ - iq_0 [e_0 \phi_2 + e_1 \phi_1 + e_2 \phi_0] \left[\epsilon F'_0 + \mathcal{O}(\epsilon^{\frac{3}{2}}) \right] - iq_0 [e_0 \phi'_0] \epsilon = 0. \end{aligned} \quad (4.36)$$

Solving at each order yields

$$\frac{dF_0}{dw} = -\frac{i}{q_0^3} = -\chi', \quad (4.37a)$$

$$\frac{dF_1}{dw} = \frac{3ie_1}{q_0^3} = 3e_1 \chi', \quad (4.37b)$$

$$\frac{1}{\overline{P}} \frac{d\overline{P}}{dw} = -\frac{4q'_0}{q_0} + \frac{3ie_2}{q_0^3} - \frac{6ie_1^2}{q_0^3}. \quad (4.37c)$$

These expressions for $F_0 = -\chi$, F_1 and \overline{P} are related to the functions χ , r_1 , and P from the late-order ansatz (4.10). First, we compare the equations for r'_1 (4.13b) and F'_1 (4.37b) to conclude that

$\frac{d}{dw} [\sqrt{2\chi}r_1 - F_1] = 0$, and thus

$$F_1(w) = \sqrt{2\chi}r_1, \quad (4.38)$$

where we have set the constant of integration so that $F_1 = 0$ at the singularity, $w = -a$, where $\chi = 0$ and $r_1 = \mu$. Also, notice from (4.13c) and (4.37c) that P and \bar{P} are related through

$$\bar{P}(w) = P(w)e^{-r_1^2(w)/4}. \quad (4.39)$$

In order to solve the inhomogeneous equation, we multiply (4.35) by the Stokes Smoothing parameter, so that $R_{\mathcal{N}} = \mathcal{S}\bar{P}e^F$, and substitute into (4.34), giving

$$- \epsilon i q_0^3 \frac{d\mathcal{S}}{dw} \bar{P} e^{F_0/\epsilon + F_1/\sqrt{\epsilon}} \sim \epsilon^{\frac{\mathcal{N}}{2}} \frac{P\Gamma\left(\frac{\mathcal{N}}{2} + \gamma\right) e^{r_1 n^{\frac{1}{2}}}}{\chi^{\frac{\mathcal{N}}{2} + \gamma}}. \quad (4.40)$$

For this expression, we write the derivative in terms of χ so that $d\mathcal{S}/dw = \chi' d\mathcal{S}/d\chi$ giving

$$\epsilon \frac{d\mathcal{S}}{d\chi} \left[\bar{P} e^{\frac{F_1}{\sqrt{\epsilon}}} \right] \sim \left[P e^{r_1 \mathcal{N}^{\frac{1}{2}}} \right] \frac{\epsilon^{\frac{\mathcal{N}}{2}} \Gamma\left(\frac{\mathcal{N}}{2} + \gamma\right) e^{\frac{\chi}{\epsilon}}}{\chi^{\frac{\mathcal{N}}{2} + \gamma}}. \quad (4.41)$$

The optimal truncation point is found where adjacent terms in the asymptotic approximation are of the same size, and thus $\epsilon^{(\mathcal{N}+1)/2} |\phi_{\mathcal{N}+1}| \sim \epsilon^{\mathcal{N}/2} |\phi_{\mathcal{N}}|$. Using the ansatz (4.10) and writing

$$\chi = r e^{i\nu} \quad (4.42)$$

we find that the optimal truncation point is found where

$$\mathcal{N} = \frac{2r}{\epsilon} + 2\rho, \quad (4.43)$$

with $\rho \in (0, 1/2)$ as $\epsilon \rightarrow 0$. Our goal now is to expand the equation for the Stokes smoothing factor, \mathcal{S} , in (4.41) in the limit $\epsilon \rightarrow 0$, and examine its rate of change as the Stokes line is crossed (a fixed r and varying ν in (4.42), which corresponds to the Stokes line $\Re(\chi) \geq 0$). We first use Stirling's formula to write

$$\Gamma(\mathcal{N}/2 + \gamma) \sim \sqrt{2\pi} \left(\frac{r}{\epsilon}\right)^{\mathcal{N}/2 + \gamma - 1/2} e^{-r/\epsilon} (1 + O(\epsilon)). \quad (4.44)$$

It next follows from the relation between r_1 and F_1 in (4.38) that

$$r_1 \mathcal{N}^{1/2} - \frac{F_1}{\sqrt{\epsilon}} = r_1 \mathcal{N}^{1/2} - \frac{\sqrt{2\chi}r_1}{\epsilon} = r_1 \sqrt{\frac{2r}{\epsilon}} \left(1 - e^{i\nu/2} + \frac{1}{2} \frac{\epsilon}{r} \rho + O(\epsilon^2)\right). \quad (4.45)$$

We can now exchange the differentiation in χ to differentiation across the Stokes line, in ν , using $d\mathcal{S}/d\chi = -(ie^{-i\nu}/r) d\mathcal{S}/d\nu$. Using the substitution (4.44) for Γ and (4.45) for r_1 in the equation for \mathcal{S} in (4.41) now yields

$$\frac{d\mathcal{S}}{d\nu} \sim i \left(\frac{P}{\bar{P}}\right) \frac{\sqrt{2\pi r}}{\epsilon^{\gamma+1/2}} e^G, \quad (4.46)$$

where we have defined G according to

$$G = -\frac{r}{\epsilon} \left(1 - e^{i\nu} + i\nu\right) + r_1 \sqrt{\frac{2r}{\epsilon}} \left(1 - e^{i\nu/2} + \frac{1}{2} \frac{\epsilon}{r} \rho + O(\epsilon^2)\right) + i\nu(1 - \rho - \gamma) \quad (4.47)$$

The first group of bracketed terms in the above expression for G indicate that the Stokes smoothing constant, \mathcal{S} , in (4.46) is exponentially small unless ν is also small. We rescale $\nu = \sqrt{\epsilon}\bar{\nu}$ and note that $G = -r\bar{\nu}^2/2 - ir_1\sqrt{r/2} + O(\sqrt{\epsilon})$. Substitution of this expression into the equation for \mathcal{S} in (4.46)

yields after simplification

$$\frac{dS}{d\bar{\nu}} \sim i \left(\frac{P}{\bar{P}} \right) \frac{\sqrt{2\pi r}}{\epsilon^\gamma} \exp \left[- \left(\sqrt{\frac{r}{2}} \bar{\nu} + i \frac{r_1}{2} \right)^2 \right] e^{-r_1^2/4}. \quad (4.48)$$

Finally, we may use the relationship between P and \bar{P} in (4.39) to conclude that

$$\frac{dS}{d\bar{\nu}} \sim i \frac{\sqrt{2\pi r}}{\epsilon^\gamma} \exp \left[- \left(\sqrt{\frac{r}{2}} \bar{\nu} + i \frac{r_1}{2} \right)^2 \right]. \quad (4.49)$$

It remains now to only substitute $\bar{\theta} = \bar{\nu} + ir_1/\sqrt{2r}$ in order to properly centre the integration over the Stokes line. Because r_1 is locally constant near the Stokes line, and because $|\chi| = r$ is fixed (by the optimal truncation) then we must have $d\bar{\theta}/d\bar{\nu} = 1 + \mathcal{O}(\sqrt{\epsilon})$. Thus,

$$\frac{dS}{d\bar{\theta}} \sim i \frac{\sqrt{2\pi r}}{\epsilon^\gamma} e^{-r\bar{\theta}^2/2}. \quad (4.50)$$

which is precisely the same expression for the Stokes smoothing that occurs for the case of well-separated singularities [11]. We integrate (4.50) from $\bar{\theta} = \infty$ to $\bar{\theta} = -\infty$, which corresponds to crossing the Stokes line as w increases [due to the geometry of the Stokes line in Figure 2 coupled with parameterization of χ in (4.42)]. We thus obtain $S \sim -2\pi i/\epsilon^\gamma$. To conclude, the remainder switched-on across Stokes lines is

$$\phi_{\text{exp}}^{\text{cc}} \equiv [R_{\mathcal{N}}]_-^+ \sim -\frac{2\pi i}{\epsilon^\gamma} [P(w)e^{-r_1^2(w)/4}] \exp \left[-\frac{\chi}{\epsilon} + \frac{F_1}{\sqrt{\epsilon}} \right] \quad (4.51)$$

moving in the direction of increasing w , and where we have used the expression for F_0 in (4.37a), and the replacement of \bar{P} by P in (4.39).

We wish to obtain an expression for $|\phi_{\text{exp}}^{\text{cc}}|$ when w is real and positive. Recall that the branch of χ was chosen in (4.14) so that $\Re(\chi) = a > 0$ for $w > 0$, which indeed corresponds to exponential decay in (4.51). Similarly, we select the branch of $F_1 = \sqrt{2\chi}r_1$ in (4.38) so that, it too, will be assured to possess a positive real value on $w > 0$. This yields

$$F_1(w) = -3\pi\beta|\sigma_2 - \sigma_1| + i[3\beta(\sigma_2 - \sigma_1)\log(w/a)], \quad (4.52)$$

where we have used r_1 in (4.15) and $f_1 = \sigma_2 - \sigma_1$.

Next, with P given in (4.32) and $\gamma = \gamma_r + i\gamma_c = 1 + i\frac{3\beta^2}{2a}(2f_1^2 - f_2)$ from (4.17), we have

$$|P(w)e^{-r_1^2(w)/4}| = |c^6 X| e^{-\frac{9\beta^2}{4a}(2f_1^2 - f_2)} \Omega^{\text{cc}} |q_0(w)|^{2(1-3\gamma)}, \quad (4.53)$$

since μ_1^2 appearing in P purely imaginary by (4.18c). Note that in the above formula, we have also used the fact that $\gamma_c \text{Arg}(c^6 X) = \gamma_c \text{Arg}(-i) = \gamma_c(3\pi/2)$. Using $|c^6 X| = a/2$ from (4.18a) and (4.18b), and combining (4.51)–(4.53), we conclude that the amplitude of the exponentially small waves is

$$|\phi_{\text{exp}}^{\text{cc}}| \sim \left[\frac{\pi a \Omega^{\text{cc}}}{\epsilon q_0^4(w)} \right] \exp \left[-\frac{9\beta^2}{4a}(2f_1^2 - f_2) \right] \exp \left[-\frac{a\pi}{\epsilon} - \frac{3\pi\beta|\sigma_2 - \sigma_1|}{\sqrt{\epsilon}} \right]. \quad (4.54)$$

5. Numerical verification of $\sigma_1 = 1/6$ and $\sigma_2 = 1/6$

We will now apply the formulae developed over the course of the previous sections to the case where q_s contains singularity powers of $\sigma_1 = 1/6$ and $\sigma_2 = 1/6$. In addition to comparing the asymptotic predictions to numerical computations, the most important behaviour to verify is that, in the limit $\beta \rightarrow 0$, the close-singularity approximation tends to the one-singularity approximation, and as $\beta \rightarrow \infty$, the close-singularity approximation tends to the two-singularity approximation. Our choice of the symmetric case of $\sigma_1 = \sigma_2 = 1/6$ helps to simplify some of the needed computations. In particular, $f_1 = 0$ and $f_2 = 1/6$.

To begin, we recall that there are two forms of the q_s function in the differential equation (2.1) of interest: the two-singularity (2.2) and single-singularity (2.3) versions given by

$$q_s = \frac{w^{1/3}}{(w + a_1)^{1/6}(w + a_2)^{1/6}} \quad \text{and} \quad q_s = \left(\frac{w}{w + a} \right)^{1/3}. \quad (5.1)$$

The well-separated case for $a_1 = a + \sqrt{\epsilon}\beta$ and $a_2 = a - \sqrt{\epsilon}\beta$ was treated in §3, whereas the uniform limit of merging singularities was treated in §4. The amplitude of the waves for both the well-separated and single-singularity case is given by (3.16), and depend on a crucial pre-factor, Ω , calculated through a numerical solution of a nonlinear recurrence relation. Both the well-separated and single-singularity variants use the same Ω , whereas the closely-separated variant requires an Ω^{cc} that depends on β . We shall write

$$\Omega(\sigma_k) \quad \text{and} \quad \Omega^{\text{cc}}(\sigma_1, \sigma_2; \beta), \quad (5.2)$$

for the two versions, and where σ_k is the local singularity power which corresponds to the generated exponential.

For the close-singularity case, the wave amplitudes are given by (4.54), and in the limit $w \rightarrow \infty$, $q_0 \rightarrow 1$, so we have

$$|\phi_{\text{exp}}^{\text{cc}}| = a \exp \left[\frac{3\pi\beta^2}{8a} \right] \Omega^{\text{cc}}\left(\frac{1}{3}; \beta\right) \left[\frac{\pi}{\epsilon} e^{-\frac{\pi a}{\epsilon}} \right]. \quad (5.3)$$

For the single-singularity case, we have $q_s \sim c(w + a)^{-1/3}$ near the singularity with $c = (-a)^{1/3}$. We thus apply the amplitude approximation (3.16) with $\sigma_k = 1/3$, $c_k = c$, and $\gamma_k = 1$, which follows from (3.8). Since the outer analysis of the close-singularity analysis involves a derivation of the singular, χ , corresponding to a single merged singularity, then the $\chi = \chi_k$ is given by (4.14), and $\Re(\chi) = a$ along the positive real axis. This yields the amplitude estimate

$$|\phi_{\text{exp}}^{\text{single}}| \sim a \Omega\left(\frac{1}{3}\right) \left[\frac{\pi}{\epsilon} e^{-\frac{\pi a}{\epsilon}} \right]. \quad (5.4)$$

Thus, in the limit $\beta \rightarrow 0$, we have $\Omega_1^{\text{cc}}\left(\frac{1}{3}; \beta\right) \rightarrow \Omega\left(\frac{1}{3}\right)$ as expected. This limiting behaviour is shown in Figure 5 for the case of $a = 0.5$ ship where we see that indeed, the close-singularity approximation tends to the one-singularity approximation as $\beta \rightarrow 0$.

We now turn to the well-separated two-singularity approximation. Here, there are two singular functions (and hence two exponentially small waves) given by

$$\chi_1(w) = \int_{-a_1}^w \frac{i}{q_s^3(\varphi)} d\varphi \quad \text{and} \quad \chi_2(w) = \int_{-a_1}^w \frac{i}{q_s^3(\varphi)} d\varphi. \quad (5.5)$$

However, it can be verified that if $\sigma_2 = 1/6$ and σ_1 approaches $1/6$ from above, then the previous Stokes line from $w = -a_1$ has flattened onto the real w axis and now lies between $-a_1 \leq w \leq -a_2$. This follows by virtue of $\chi' = i/q_s^3 > 0$ in this region. Thus, we conclude that waves are entirely generated by the singularity at $w = -a_2$. For $w > 0$, we have

$$\Re(\chi_2) = \Re \left(\int_{-a_2}^{-a_1} + \int_{-a_1}^w \right) \frac{i}{q_s^3(\varphi)} d\varphi = \pi a - \pi a \sqrt{1 - \epsilon(\beta/a)^2}, \quad (5.6)$$

where the first term on the right hand-side follows from $\Re(\chi_1) = \pi(a_1 + a_2)/2 = \pi a$ from a residue contribution at infinity. Thus, the wave from the small perturbation about the point $w = -a$ has produced an additional exponential factor of $e^{\pi\beta^2/2a}$.

With $q_s \sim c_2(w + a_2)^{\sigma_2}$ near the singularity, we obtain values of

$$\sigma_2 = 1/6, \quad c_2 = \frac{a^{\frac{1}{3}} e^{\pi i/3}}{(2\sqrt{\epsilon}\beta)^{\frac{1}{6}}}, \quad \gamma_2 = 2/3 \quad (5.7)$$

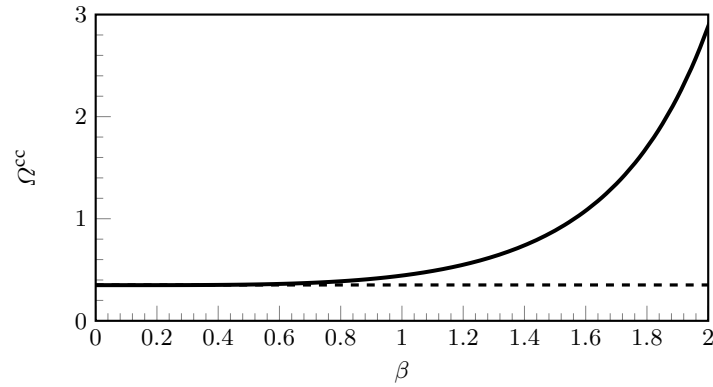


FIGURE 5: The solid curve is the pre-factor $\Omega^{\text{cc}}(1/6, 1/6; \beta)$ for the close-singularity problem, with $a = 0.5$. As $\beta \rightarrow 0$ and the two singularities coalesce, the pre-factor approaches the same value as for the one-singularity case, with $\Omega(1/3) \approx 0.351$ (shown dashed).

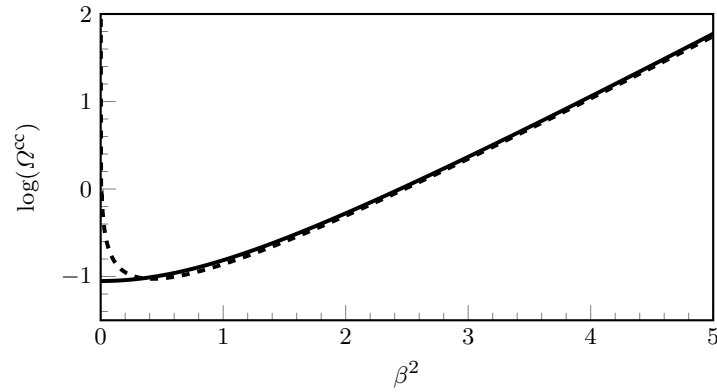


FIGURE 6: The solid curve is the pre-factor $\Omega^{\text{cc}}(1/6, 1/6; \beta)$ for close-singularity approximation, with $a = 0.5$. As $\beta \rightarrow \infty$ and the singularities separate, the pre-factor approaches the dashed curve with $\Omega(1/6) \times 2[a/(9\beta^2)]^{1/3} \exp[\pi\beta^2/3a]$, corresponding to the well-separated result.

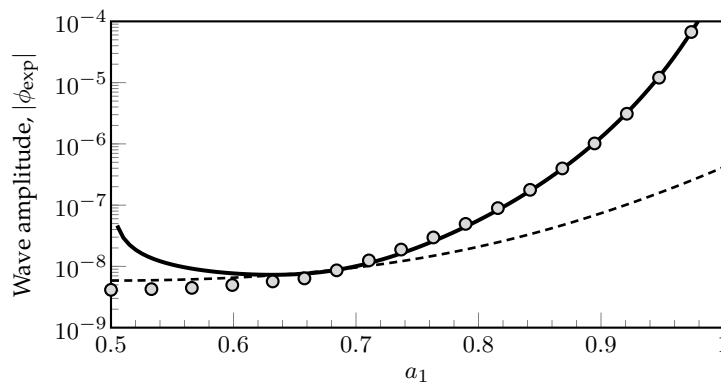


FIGURE 7: The numerical solution (nodes) for the $\sigma_1 = \sigma_2 = 1/6$ forcing versus the asymptotic approximations for $\epsilon = 0.075$ and $a_1 + a_2 = 1$. The two-singularity approximation (solid line) is singular when $a_1, a_2 \approx 0.5$ near the left. Here, the solution is well approximated by the close-singularity approximation (dashed).

where γ_2 follows from (3.8). Using (5.6) in (3.16), we see that the amplitude of the exponentially small waves from the well-separated analysis yields

$$|\phi_{\text{exp}, 2}| \sim \frac{2a^{\frac{4}{3}} e^{\frac{\pi\beta^2}{2a}}}{(3\beta)^{\frac{2}{3}}} \Omega\left(\frac{1}{6}\right) \left[\frac{\pi}{\epsilon} e^{-\frac{\pi a}{\epsilon}} \right]. \quad (5.8)$$

Now comparing with the close-singularity approximation in (5.3), we see that in order to match with (5.8) in the limit $\beta \rightarrow \infty$, we require

$$\Omega^{\text{cc}}\left(\frac{1}{6}, \frac{1}{6}; \beta\right) \sim 2 \left(\frac{a}{9\beta^2} \right)^{1/3} e^{\frac{\pi\beta^2}{8a}} \Omega\left(\frac{1}{6}\right). \quad (5.9)$$

In Figure 6, we plot the natural logarithms of the left and right-hand sides of (5.9) as a function of β^2 and indeed, the convergence between the two values is very fast.

The final result is shown in Figure 7; here, we compare the numerical and asymptotic approximations for far field wave amplitudes of the $\sigma_1 = \sigma_2 = 1/6$ forcing. As expected, the two-singularity approximation of (5.8) for the wave amplitude is a fine approximation, but only until the two singularities begin merging near $a_1 = a_2 = 0.5$. At this point, the close-singularity approximation of (5.3) provides a much better match to the numerical results.

6. Discussion

To summarize: in this paper, we proposed a model singularly perturbed differential equation that was inspired studies on water waves and ship hydrodynamics [13]. However, for this toy model, the divergence of the late terms of the associated asymptotic expansion was not described through the common factorial-over-power ansatz (Dingle [1]), but instead through a more general exponential-over-power ansatz. By applying methods in exponential asymptotics, optimally truncating the series, and smoothing the Stokes line, we were able to recover the exponentially small waves switched on.

Now in regards to the original motivation of water waves and hydrodynamics, the limit of coalescing singularities represents a rather niche area of practical interest; indeed, one would argue that the effort to derive the final exponential $\phi_{\text{exp}}^{\text{cc}}$ in (4.54) far exceeds the effort to numerically solve the differential equation directly! However, the more important lesson from this work is in relation to the general class of nonlinear problems, $\Re(z, y; \epsilon) = F$, introduced in (1.7). For such problems where the solution of the differential equation is forced by two interleaving asymptotic expansions [e.g. the expansion resulting from the ϵ forcing in (2.1), and the expansion resulting from the $\epsilon^{\ell/m}$ in (4.3)], we must expect the use of more generalized exponential-over-power divergence. Our methodology in this paper highlights several interesting aspects of the adjusted exponential asymptotics theory, including the merging of multiple Stokes lines in an outer region, combined with a thickening of such lines during the optimal truncation procedure.

We may also ask the question of why such exponential-over-power divergence has not been necessary for similar problems of coalescing singularities in the exponential asymptotics literature. This situation of interleaving terms also arises in the Saffman-Taylor viscous fingering problem (see for example, [23] and [24]). If we follow the same ideas as presented there, then we would expect our expansion for ϕ to split into m sub-expansions:

$$\begin{aligned} \phi = & \left[\phi_0 + \epsilon^{\frac{1}{m}} \phi_1 + \epsilon^{\frac{2}{m}} \phi_2 + \dots \right] + \sum_{n=n^*}^{\infty} \epsilon^n \phi_{mn} + \sum_{n=n^*}^{\infty} \epsilon^{n+\frac{1}{m}} \phi_{mn+1} \\ & + \dots + \sum_{n=n^*}^{\infty} \epsilon^{n+\frac{k}{m}} \phi_{mn+k} + \dots + \sum_{n=n^*}^{\infty} \epsilon^{n+\frac{m-1}{m}} \phi_{mn+m-1}. \end{aligned} \quad (6.1)$$

The bracketed terms are the early orders. Our interest is in deriving the form of the high-order terms, given by ϕ_{nm+k} for $k = 0, 1, \dots, m-1$ as $n \rightarrow \infty$, which we claim can be represented using m distinct ansatzes.

However, the Saffman-Taylor problem turns out to be simpler because the late-order terms are only coupled a distance $\mathcal{O}(\epsilon)$ apart. In other words, for that problem, as $n \rightarrow \infty$, the leading-order behaviour of ϕ_{mn} in (6.1) only depends on terms within its own sub-expansion. Because of this unique property, the late terms of the Saffman-Taylor problem are still given by a factorial over power ansatz. This simplification does not hold for our problem.

There exist other distinguished limits that may yield interesting results or alternative methodologies. For instance, what occurs when σ_1 and σ_2 in (2.2) vary as $\epsilon \rightarrow 0$? Since the values of σ_1 and σ_2 determine the behaviour of the singulants, χ_k in (3.5) near the singularities, changing these powers changes the Stokes line configurations in the complex plane. There are indeed limitations of our methodology (also noted in [13]) where if the σ_1 and σ_2 are not rational numbers, then the asymptotics procedure becomes more difficult. Indeed, in some situations, it may be important to understand how σ_1 and σ_2 continuously approach some special value as $\epsilon \rightarrow 0$. For instance, Lustri *et al.* [25] study free-surface flow over an inclined step where the bottom topography is designed in order to produce downstream wave cancellation (to leading order). However, as the geometry approached this optimized configuration (by varying the inclination angle in the step), they noted an interesting behaviour where the Stokes line contribution from the two singularities (the stagnation point and corner in the step) rapidly oscillated in and out of phase. This variant of the close-singularities problem will present an interesting problem for future work.

References

- 1 Dingle, R. B. 1973 *Asymptotic Expansions: Their Derivation and Interpretation*. Academic Press, London.
- 2 Berry, M. 1991 Asymptotics, superasymptotics, hyperasymptotics... In *Asymptotics beyond all orders* (ed. H. Segur), pp. 1–14. Springer.
- 3 Berry, M. V. 1989 Uniform asymptotic smoothing of Stokes discontinuities. *Proc. Roy. Soc. London*, **A 422**, 7–21.
- 4 Meyer, R. E. 1989 A simple explanation of the Stokes phenomenon. *SIAM Review*, **31**(3), 435–445.
- 5 Olde Daalhuis, A. B., Chapman, S. J., King, J. R., Ockendon, J. R. & Tew, R. H. 1995 Stokes Phenomenon and matched asymptotic expansions. *SIAM J. Appl. Math.*, **55**(6), 1469–1483.
- 6 Bleistein, N. & Handelsman, R. A. 1975 *Asymptotic expansions of integrals*. Courier Dover Publications.
- 7 Chapman, S. J., King, J. R. & Adams, K. L. 1998 Exponential asymptotics and Stokes lines in nonlinear ordinary differential equations. *Proc. R. Soc. Lond. A*, **454**, 2733–2755.
- 8 Baker, G. A. 1975 *Essentials of Padé Approximants*. Academic Press, New York.
- 9 Henrici, P. 1977 Applied and computational complex analysis: Special functions-integral transforms-asymptotics-continued fractions, volume 2. *AMC*, **10**, 12.
- 10 Chapman, S. J. & Vanden-Broeck, J.-M. 2002 Exponential asymptotics and capillary waves. *SIAM J. Appl. Math.*, **62** (6), 1872–1898.
- 11 Chapman, S. J. & Vanden-Broeck, J.-M. 2006 Exponential asymptotics and gravity waves. *J. Fluid Mech.*, **567**, 299–326.
- 12 Trinh, P. H., Chapman, S. J. & Vanden-Broeck, J.-M. 2011 Do waveless ships exist? Results for single-cornered hulls. *J. Fluid Mech.*, **685**, 413–439. doi:10.1017/jfm.2011.325.
- 13 Trinh, P. H. & Chapman, S. J. 2014 The wake of a two-dimensional ship in the low-speed limit: results for multi-cornered hulls. *J. Fluid Mech.*, **741**, 492–513. doi:10.1017/jfm.2013.589.
- 14 Trinh, P. H. & Chapman, S. J. 2013 New gravity-capillary waves at low speeds. Part 1: Linear theory. *J. Fluid Mech.*, **724**, 367–391. doi:10.1017/jfm.2013.110.
- 15 Trinh, P. H. & Chapman, S. J. 2013 New gravity-capillary waves at low speeds. Part 2: Nonlinear theory. *J. Fluid Mech.*, **724**, 392–424. doi:10.1017/jfm.2013.110.
- 16 Trinh, P. H. 2010 *Asymptotic Methods in Fluid Mechanics: Survey and Recent Advances*, chap. Exponential Asymptotics and Stokes Line Smoothing for Generalized Solitary Waves, pp. 121–126. SpringerWienNewYork.

- 17 Boyd, J. P. 1998 *Weakly nonlocal solitary waves and beyond-all-orders asymptotics*. Kluwer Academic Publishers.
- 18 Olde Daalhuis, A. B. 1999 On the computation of Stokes multipliers via hyperasymptotics. Resurgent functions and convolution integral equations. *Surikaiseikikenkyusho Kokyuroku*, (1088), 68–78.
- 19 Costin, O. 2008 *Asymptotics and Borel summability*, vol. 141. Chapman & Hall/CRC.
- 20 Grimshaw, R. 2010 *Asymptotic Methods in Fluid Mechanics: Survey and Recent Advances*, chap. Exponential Asymptotics and Generalized Solitary Waves, pp. 71–120. SpringerWienNewYork.
- 21 Tuck, E. O. 1991 Ship-hydrodynamic free-surface problems without waves. *J. Ship Res.*, **35**(4), 277–287.
- 22 Van Dyke, M. 1975 *Perturbation Methods in Fluid Mechanics: By Milton Van Dyke. Annotated Ed.* Parabolic Press.
- 23 Combescot, R., Hakim, V., Dombre, T., Pomeau, Y. & Pumir, A. 1988 Analytic theory of the Saffman-Taylor fingers. *Phys. Rev. A*, **37**(4), 1270–1283.
- 24 Chapman, S. J. 1999 On the role of Stokes lines in the selection of Saffman-Taylor fingers with small surface tension. *Eur. J. Appl. Math.*, **10**(6), 513–534.
- 25 Lustri, C. J., McCue, S. W. & Binder, B. J. 2012 Free surface flow past topography: A beyond-all-orders approach. *Eur. J. Appl. Math.*, **1**(1), 1–27.
- 26 Vanden-Broeck, J.-M. 2010 *Gravity-Capillary Free-Surface Flows*. Cambridge, UK: Cambridge University Press.
- 27 Xie, X. & Tanveer, S. 2002 Analyticity and nonexistence of classical steady Hele-Shaw fingers. *Commun. Pur. Appl. Math.*, **56**(3), 353–402.

A. Relationship to nonlinear equations of potential flow

Consider steady, incompressible, irrotational, and inviscid flow in the presence of gravity and past a semi-infinite body, which consists of a flat bottom and a piecewise linear front face. The dimensional problem can be reposed in terms of a non-dimensional boundary-integral formulation in the potential (ϕ, ψ) -plane. The unknowns are the fluid speed $q = q(\phi, \psi)$, and streamline angles, $\theta = \theta(\phi, \psi)$, measured from the positive x -axis. The body and free-surface is given by the streamline $\psi = 0$, and we assume the free-surface ($\phi > 0$) attaches to the hull ($\phi < 0$) at a stagnation point. The free-surface, with $\psi = 0$, is then obtained by solving a boundary-integral equation, coupled with Bernoulli's condition:

$$\log q = \log q_s + \frac{1}{\pi} \int_0^\infty \frac{\theta(\varphi)}{\varphi - \phi} d\varphi \quad (\text{A } 1a)$$

$$\epsilon q^2 \frac{dq}{d\phi} = -\sin \theta, \quad \text{on } \varphi = 0, \quad (\text{A } 1b)$$

where $\epsilon = U^3/gK$ is related to the square of the Froude draft number with upstream flow U , gravity g , and potential length scale, K . The function $q_s = q_s(\phi)$ is calculated through

$$\log q_s \equiv \frac{1}{\pi} \int_{-\infty}^0 \frac{\theta(\varphi)}{\varphi - \phi} d\varphi, \quad (\text{A } 2)$$

and for a surface-piercing object such as a ship, it is assumed that this function is known through the specification of the angle, θ , along the negative real ϕ -axis, which corresponds to the geometry of the hull. For instance, a semi-infinite ship hull with a single corner at $\phi = -a$ and with a face of angle $\pi\sigma$ is given by the q_s in (2.3). Similarly, the two-singularity q_s in (2.2) corresponds to a two-cornered hull with angles $\pi\sigma_1$ and $\pi\sigma_2$. See [12, 13] for more details on the derivation of (A 1a) and (A 1b) as it pertains to the ship problem. For a more detailed reference on boundary integral equations for free-surface flows, see Vanden-Broeck [26].

In the exponential asymptotics framework, we are interested in studying the analytic continuation of the free-surface and thus allowing $q(\phi, 0) \mapsto q(w)$ and $\theta(\phi, 0) \mapsto \theta(w)$ to be complex

functions of the complex potential, $\phi + i0 \mapsto w$. However, in previous exponential asymptotic studies of the boundary integral equations of potential flow, it has been shown that because the exponential switched-on across Stokes line is almost exclusively determined by the local behaviour of the solution near the singularities in the complex plane (far away from where the boundary integral is evaluated), then the integral can be dropped from the analysis with little consequence to the methodology. This simplification is discussed in more within [12], and is argued rigorously for the related problem of Saffman-Taylor viscous fingering in the work of Xie and Tanveer [27].

In fact, it can be shown that the integral term serves to only change the amplitude coefficient of the waves [e.g. (4.54)] by a non-zero $\mathcal{O}(1)$ factor. This way, we simplify the full problem in (A 1) to a simpler nonlinear differential equation in q . Analytic continuation into the upper-half plane then gives an initial value problem

$$\epsilon q_s q^3 \frac{dq}{dw} + \frac{i}{2} [q^2 - q_s^2] = 0, \quad q(0) = 0, \quad (\text{A } 3)$$

where now q is a complex-valued function, and the physical fluid boundary is identified with $w \in \mathbb{R}^+$. The boundary condition $q(0) = 0$ imposes a stagnation point attachment between the free-surface and solid boundary. Substitution of $\phi = q^2$ (note this ϕ is distinct from the fluid potential ϕ introduced earlier) leads to the main differential equation of this paper (2.1).

B. General methodology for the close-singularity analysis

In the paper, we principally studied the differential equation (2.1) subject to the two-singularity forcing, q_s , in (2.2) where $\sigma_1 + \sigma_2 = 1/3$. These values were chosen so that the series asymptotic expansion of q_s (in powers of $\sqrt{\epsilon}$) interleaves in the simplest non-trivial way with the usual ϵ expansion from the differential equation (2.1). Other combinations of $\sigma_1 + \sigma_2$ will produce more complicated interleaving behaviour, and hence more complicated exponential-over-power divergence. In this section, we review some of the main ideas of how the methodology is extended to the general problem.

Rather than beginning with the outer analysis (far from singularities) as we have in §4, we will begin instead with the inner analysis, since it is easier to see the emergence of the correct divergent ansatz in this regime.

(i) Inner analysis with $w + a = \mathcal{O}(\epsilon^{\ell/m})$

Our plan is to derive the leading-order inner problem, and then obtain the correct form of the solution as we tend to the outer region. Writing $q_0 = [w/(w+a)]^\sigma$ for the merged forcing function in (4.2), we note that as $w \rightarrow -a$, $q_s \sim c(w+a)^{-\sigma}$, where $c = (-a)^\sigma$, and $\sigma = \sigma_1 + \sigma_2$. The inner variables, z and $\hat{\phi}$, are defined using

$$w + a = (\epsilon/X)^{\ell/m} z^\ell, \quad \phi = c^2 (w+a)^{-2\sigma} \hat{\phi}. \quad (\text{A } 1)$$

where we have written $X = i/[c^3(1+3\sigma)]$. The constants c and X are introduced to simplify the algebra. From (2.1), the inner equation then becomes

$$\frac{1}{mz^m} \left[-2\sigma \ell \hat{q}_s \hat{\phi}^2 + z \hat{q}_s \hat{\phi} \frac{d\hat{\phi}}{dz} \right] + [\hat{\phi} - \hat{q}_s^2] = 0. \quad (\text{A } 2)$$

In (A 2), we have written $q_s = q_0 \hat{q}_s$, and from (4.3),

$$\hat{q}_s = \frac{(X^{-\ell/m} z^\ell)^{\sigma_1 + \sigma_2}}{(z^\ell + \beta)^{\sigma_1} (z^\ell - \beta)^{\sigma_2}} \equiv \sum_{n=0}^{\infty} \frac{\hat{e}_n}{z^n}, \quad (\text{A } 3a)$$

where we have defined

$$\hat{e}_n = \begin{cases} \beta^{n/\ell} X^{n/m} f\left(\frac{n}{\ell}\right) & \text{if } \text{mod}(n, \ell) = 0 \\ 0 & \text{if } \text{mod}(n, \ell) \neq 0. \end{cases} \quad (\text{A } 3b)$$

We wish to study the leading-order solution, $\hat{\phi}$, as it tends outwards. Thus as $z \rightarrow \infty$, we substitute $\hat{\phi} = \sum_{n=0}^{\infty} A_n/z^n$ into the inner equation (A 2), giving

$$A_0 = 1, \quad A_n = \sum_{j=0}^n \hat{e}_j \hat{e}_{n-j} \quad \text{for } n < m, \quad (\text{A } 4a)$$

$$A_n = \sum_{j=0}^n \hat{e}_j \hat{e}_{n-j} + \sum_{k=0}^{n-m} \hat{e}_k \left[\sum_{j=0}^{n-m-k} \left(\frac{j+2\sigma\ell}{m} \right) A_j A_{n-m-k-j} \right]. \quad \text{for } n \geq m, \quad (\text{A } 4b)$$

A simple numerical computation assures us that A_n diverges in the limit $n \rightarrow \infty$, and indeed, the form of the late terms follows

$$A_n \sim \Omega^{\text{cc}} e^{i\tau} \Gamma\left(\frac{n}{m} + \gamma\right) \exp\left[\sum_{j=1}^{m-1} \mu_j n^{\frac{m-j}{m}}\right], \quad (\text{A } 5)$$

as $n \rightarrow \infty$, with $\gamma, \mu_j \in \mathbb{C}$, $\Omega^{\text{cc}}, \tau \in \mathbb{R}$. Like the discussion surrounding (4.24), we caution the reader that the form of (A 5) may need to be multiplied by $(-1)^n$ depending on the form of (A 5). The special case of $\mu_j \equiv 0$ for all j corresponds to the more typical case of factorial divergence, which is observed for most problems in exponential asymptotics. The suitability of (A 5) can be understood by dividing (A 4b) by A_n and writing it as

$$1 + \sum_{j=0}^m \left[\sum_{k=0}^j \left(-\frac{1}{m}\right) \hat{e}_k A_{j-k} \right] \frac{n A_{n-m-j}}{A_n} + \left[\frac{(4\ell - m) \hat{e}_0 A_0}{3m} \right] \frac{A_{n-m}}{A_n} + \dots = 0 \quad (\text{A } 6)$$

Then using the ansatz (A 5), we can see that the series expansions of the various ratios appearing in (A 6) are given by

$$\begin{array}{rcl} \frac{A_{n-m}}{A_n} & \sim & \frac{c_{10}}{n} + \frac{c_{11}}{n^{\frac{m+1}{m}}} + \dots + \frac{c_{1(m-1)}}{n^{\frac{2m-1}{m}}} + \frac{c_{1m}}{n^2} \\ \frac{A_{n-m-1}}{A_n} & \sim & \frac{c_{21}}{n^{\frac{m+1}{m}}} + \dots + \frac{c_{2(m-1)}}{n^{\frac{2m-1}{m}}} + \frac{c_{2m}}{n^2} \\ \vdots & & \ddots \\ \frac{A_{n-2m+1}}{A_n} & \sim & \dots + \frac{c_{(m-1)(m-1)}}{n^{\frac{2m-1}{m}}} + \frac{c_{(m-1)m}}{n^2} \\ \frac{A_{n-2m}}{A_n} & \sim & \dots + \frac{c_{mm}}{n^2}, \end{array}$$

where the factors c_{jk} are functions of μ_j and γ and in general, require the higher-order terms of Stirling's Approximation to the Gamma function.

Thus, when we search for the $n \rightarrow \infty$ limit in (A 4b), we will need to conserve the terms with factors of A_n and A_{n-m} , and terms of orders $n A_{n-m}$ to $n A_{n-2m}$. Terms with other indices will be of lower order. Then, for equation (A 6) and using the ansatz, the leading order behaviour at $\mathcal{O}(n^{-1})$ is automatically satisfied by the Gamma function; μ_1 is then determined at $\mathcal{O}(n^{-\frac{m+1}{m}})$, μ_2 is determined at $\mathcal{O}(n^{-\frac{m+2}{m}})$, and so on until μ_{m-1} is determined at $\mathcal{O}(n^{-\frac{2m-1}{m}})$. Lastly, the constant γ is determined at $\mathcal{O}(n^{-2})$. The prefactor $\Omega^{\text{cc}} e^{i\tau}$ can then be found by numerically solving the recurrence relation in (A 4b).

(ii) Outer analysis with $w + a = \mathcal{O}(1)$

We are now in a position to return to the outer equation of (2.1). Upon substituting the expansion $\phi = \sum \epsilon^n \phi_n$ into the equation, the first m terms are

$$\phi_0 = q_0^2, \quad \phi_n = q_0^2 \sum_{k=0}^n e_k e_{n-k} \quad \text{for } n < m, \quad (\text{A } 7)$$

and motivated by the form of the inner ansatz (A 5), we assume that as $n \rightarrow \infty$, the late terms are given by

$$\phi_n \sim \frac{P(w)\Gamma\left(\frac{n}{m} + \gamma\right)}{[\chi(w)]^{\frac{n}{m} + \gamma}} \exp\left[\sum_{i=1}^{m-1} r_i(w)n^{\frac{m-i}{m}}\right], \quad (\text{A } 8)$$

for complex functions χ , r_i , and P , and constant γ . Substitution of this ansatz into the differential equation yields a similar procedure to that which we used for the inner equation, except that now, we wish to keep terms ϕ_n and ϕ_{n-m} , as well as derivatives ϕ'_{n-m} to ϕ'_{n-2m} . The relevant terms at $\mathcal{O}(\epsilon^{\frac{n}{m}})$ are then

$$\phi_n + \sum_{j=0}^m \left[\sum_{k=0}^j (-iq_0) e_k \phi_{j-k} \right] \phi'_{n-m-j} + \left[(-i)e_0 \phi'_0 \right] \phi_{n-m} + \dots = 0. \quad (\text{A } 9)$$

As $n \rightarrow \infty$, the leading-order terms involve $\phi_n + (-iq_0)e_0\phi_0\phi'_{n-m} = 0$, with $e_0 = 1$ and $\phi_0 = q_0^2$. Thus the equation for χ is

$$\chi(w) = \int_{-a}^w \frac{i}{q_0^3(\varphi)} d\varphi, \quad (\text{A } 10)$$

The subsequent orders each yield first-order differential equations for $r_i(w)$ and $P(w)$. In order to match with the form of the inner ansatz in (A 5), we require $r_i(-a) = \mu_i$. Once the boundary conditions on $r_i(w)$ are imposed, the value of γ can be verified by setting $n = 0$ in the late-orders ansatz and matching its behaviour as $w \rightarrow -a$. This will turn out to be the same γ computed directly from the inner analysis.

(iii) Optimal truncation and Stokes smoothing

Once the late-order terms, ϕ_n , have been found, we can re-scale near the Stokes lines and derive the exponential switchings. We begin by truncating the asymptotic expansion at $n = \mathcal{N}$,

$$\phi = \sum_{n=0}^{\mathcal{N}-1} \epsilon^{\frac{n}{m}} \phi_n + R_{\mathcal{N}} \quad (\text{A } 11)$$

and substitute this expression into (2.1). This gives a linear equation for the remainder, $R_{\mathcal{N}}$, as well as a single $\mathcal{O}(\epsilon^{\mathcal{N}/m})$ term:

$$\mathcal{L}(R_{\mathcal{N}}; \epsilon) \sim \epsilon^{\mathcal{N}/m} \phi_{\mathcal{N}}, \quad (\text{A } 12)$$

where the relevant terms of the linear operator \mathcal{L} are given by

$$\mathcal{L}(R_{\mathcal{N}}; \epsilon) = R_{\mathcal{N}} + \sum_{j=0}^m \left[\sum_{k=0}^j (-iq_0) e_k \phi_{j-k} \right] \epsilon^{1+\frac{j}{m}} \frac{dR_{\mathcal{N}}}{dw} + \left[(-i)e_0 \phi'_0 \right] \epsilon R_{\mathcal{N}} + \dots = 0. \quad (\text{A } 13)$$

Examine now Table 1, which summarises the connection between the inner, outer, and Stokes Smoothing procedures. To review: the table shows that for the inner analysis, seeking the $n \rightarrow \infty$ limit for A_n involves equations in orders of $n^{-1/m}$; for the outer analysis, the $n \rightarrow \infty$ limit also involves equations in orders of $n^{-1/m}$; for the Stokes smoothing procedure, the exponential behaviour of $R_{\mathcal{N}}$ is determined by matching at orders in $\epsilon^{1/m}$. The equations at each order are not the same for all three analyses, but they share corresponding values near the inner region (between terms A_n and ϕ_n) and near the Stokes line (between terms ϕ_n and $R_{\mathcal{N}}$).

Before we solve the inhomogeneous equation (A 12), we first seek the homogeneous solutions of $\mathcal{L} = 0$. We expand the remainder as

$$R_{\mathcal{N}} = \bar{P}(w) \exp[F(w)] = \bar{P}(w) \exp\left[\sum_{j=0}^{m-1} \frac{F_j(w)}{\epsilon^{\frac{j}{m}}}\right]. \quad (\text{A } 14)$$

Substitution into $\mathcal{L} = 0$ yields equations at $\mathcal{O}(1)$, $\mathcal{O}(\epsilon^{\frac{1}{m}})$, \dots , $\mathcal{O}(\epsilon^{\frac{m-1}{m}})$, $\mathcal{O}(\epsilon)$, which determines F'_0 , F'_1 , \dots , F'_{m-1} , and \bar{P} , each in turn.

| REGION | FORM | FIRST | FIRST | SECOND | ... | LAST | LAST |
|--------|--|-------------------|---|---|---------|---|-----------------------------|
| Inner | $\sum_n \frac{A_n}{z^n}$ | A_n | nA_{n-m} | nA_{n-m-1} | \dots | nA_{n-2m} | A_{n-m} |
| Outer | $\sum_n \epsilon^{\frac{n}{m}} \phi_n$ | ϕ_n | ϕ'_{n-m} | ϕ'_{n-m-1} | \dots | ϕ'_{n-2m} | ϕ_{n-m} |
| Stokes | $R_{\mathcal{N}} e^F$ | $R_{\mathcal{N}}$ | $\epsilon^{\frac{1}{m}} R'_{\mathcal{N}}$ | $\epsilon^{\frac{2}{m}} R'_{\mathcal{N}}$ | \dots | $\epsilon^{\frac{m-1}{m}} R'_{\mathcal{N}}$ | $\epsilon R'_{\mathcal{N}}$ |

TABLE 1: Connection between inner, outer, and Stokes line analyses.

To solve the inhomogeneous equation (A 12), we multiply the homogeneous solution (A 14) by the Stokes smoothing factor \mathcal{S} , then substitute $R_{\mathcal{N}} = S\bar{P} \exp[F(w)]$ this expression into (A 12), giving

$$- \epsilon i q_0^3 \frac{d\mathcal{S}}{dw} \bar{P} e^F \sim \epsilon^{\mathcal{N}/m} \phi_{\mathcal{N}}, \quad (\text{A } 15)$$

where the bracketed factor corresponds to the $j = 0$ contribution from the summation in (A 13). Finally, we can establish a relationship between the components of the final exponential given by $R_{\mathcal{N}}$, and the numerical constant of the inner problem Ω^{cc} , all related through the late-order terms r_i and P . Simplification of (A 15) will then provide an equation for the value of \mathcal{S} across the Stokes line.